

Chapter 17

Multiple Quantum Spectroscopy of Liquid Samples

Timothy J. Norwood[†]

Leicester University, UK

17.1 Introduction	221
17.2 Correlation Experiments	222
17.3 Multiple Quantum Editing Experiments	224
17.4 Determination of the Sign of Scalar Coupling Constants	229
17.5 Correlation of External Random Magnetic Fields	230
References	230

17.1 INTRODUCTION

Multiple quantum coherence^{1–3} is widely used in the spectroscopy of liquid samples. Its main uses can, broadly speaking, be grouped into two categories: the encoding of chemical shift in multidimensional correlation experiments, and the editing of both one-dimensional and multidimensional spectra. Multiple quantum coherence also has several less widely used applications, including scalar coupling constant sign determination and the investigation of

the extent of correlation between external random magnetic fields. Herein will be described the properties of multiple quantum coherence, the construction of experiments, and its applications for liquid samples.

Multiple quantum coherences are those coherences for which $\Delta m_T \neq \pm 1$. Unlike single quantum coherence, multiple quantum coherence cannot either be excited directly by the application of a single nonselective rf pulse to the equilibrium magnetization of a spin system, nor detected directly since it has no net magnetization associated with it. Both excitation and detection must therefore be achieved indirectly using a sequence of rf pulses. Despite these drawbacks, multiple quantum coherences play an important role in the spectroscopy of liquid samples because their properties are both different from and complementary to those of single quantum coherence. The chemical shift of a multiple quantum coherence is a linear combination of those of its active spins k :

$$\omega_{\text{MQC}} = \sum_k \omega_k \Delta m_k \quad (17.1)$$

Multiple quantum coherences do not exhibit scalar couplings between their active spins. The scalar coupling of a MQC to a passive spin l is the linear combination of the scalar couplings of the individual active spins to the passive spin:

$$J_{\text{MQC}} = \sum \Delta m_k J_{kl} \quad (17.2)$$

[†]deceased 12 November 1999.

The relaxation properties of multiple quantum coherences are also distinct from those of the single quantum coherences of their active spins.^{1,3} However, individual expressions depend on the number of interacting spins considered.

In high-resolution spectroscopy of liquids, multiple quantum coherence is most commonly excited with a sequence of two nonselective pulses separated by a delay, which may contain a refocusing pulse. A commonly used excitation sequence is³

$$90_x^\circ - \frac{\tau}{2} - 180_y^\circ - \frac{\tau}{2} - 90_\phi^\circ$$

where $\phi = x$ to excite even orders of coherence, and $\phi = y$ to excite odd orders. Typically, $\tau < 1/(2J)$; the exact value used depends on the application. The effect of this pulse sequence, when $\phi = x$ and $\tau = 1/(2J)$, on the magnetization of a spin k coupled to a spin l is sketched below in the product operator formalism:⁴

$$I_{kz} \xrightarrow{90_x^\circ} -I_{ky} \xrightarrow{\tau} 2I_{kx}I_{lz} \xrightarrow{90_x^\circ} -2I_{kx}I_{ly}$$

where $2I_{kx}I_{ly}$ is a linear combination of zero quantum and double-quantum coherence with active spins k and l . The components of pure zero quantum coherence (ZQC) and double quantum (DQC) are given by linear combinations of two-spin product operators:

$$(ZQC)_x = \frac{1}{2}(2I_{kx}I_{lx} + 2I_{ky}I_{ly}) \quad (17.3)$$

$$(ZQC)_y = \frac{1}{2}(2I_{kx}I_{ly} - 2I_{ky}I_{lx}) \quad (17.4)$$

$$(DQC)_x = \frac{1}{2}(2I_{kx}[I_{lx} - 2I_{ky}[I_{ly}]) \quad (17.5)$$

$$(DQC)_y = \frac{1}{2}(2I_{kx}[I_{ly} + 2I_{ky}[I_{lx}]) \quad (17.6)$$

Detection is, in essence, the reverse of excitation; a single 90° pulse will usually convert a component of multiple quantum coherence into antiphase single quantum coherence. This can be allowed to become in-phase prior to acquisition, if desired, by the subsequent incorporation of a spin echo into the pulse sequence. As with single quantum experiments, the desired coherence transfer pathways in a multiple quantum experiment can readily be selected using either phase cycling or magnetic field gradient pulses.³

homonuclear or heteronuclear. This distinction is important because the motivation for using the two types of experiment is usually quite different.

In homonuclear correlation experiments multiple quantum coherence is used for one or more of three reasons:

1. Multiple quantum coherences provide alternative spectral dispersions to those of single quantum coherence. Peaks that overlap in a “conventional” correlation spectrum such as COSY may be resolved in a multiple quantum correlation spectrum. In addition, high-order multiple quantum correlation spectra contain relatively few peaks.
2. Spectra may contain peaks that provide relay-type information, i.e. peaks which correlate pairs of spins which, while not coupled to each other, are both coupled to a common third spin.
3. Spectra of orders greater than 2 do not contain autocorrelation peaks. Autocorrelation peaks often hide cross correlations between spins with similar chemical shifts, and which consequently occur close to the diagonal of the COSY spectrum. This problem can be particularly severe in spectra of nuclei with low natural abundance, where autocorrelation peaks may be several orders of magnitude more intense than cross-correlation peaks.

Multiple quantum coherence has found widespread use in heteronuclear correlation spectroscopy. Although it is not used to encode a multiple quantum frequency, it is used as a tool of convenience for encoding the single quantum chemical shift of one of the active spins. For reasons of sensitivity, in heteronuclear correlation experiments the nucleus with the highest magnetogyric ratio is usually both excited and detected; this is known as “inverse detection”. A typical purely single quantum pulse sequence for inversely detected heteronuclear correlation spectroscopy requires 10 pulses, while its multiple quantum analogue contains only four. By minimizing the number of pulses in a sequence, one minimizes both the amount of signal lost due to pulse imperfections, and the length of the phase cycle that must be used to obtain a clean spectrum.

17.2 CORRELATION EXPERIMENTS

Multiple quantum coherence correlation experiments can be categorized according to whether they are

17.2.1 Homonuclear Correlation Experiments

Although many homonuclear multiple quantum correlation experiments have been proposed, very few of

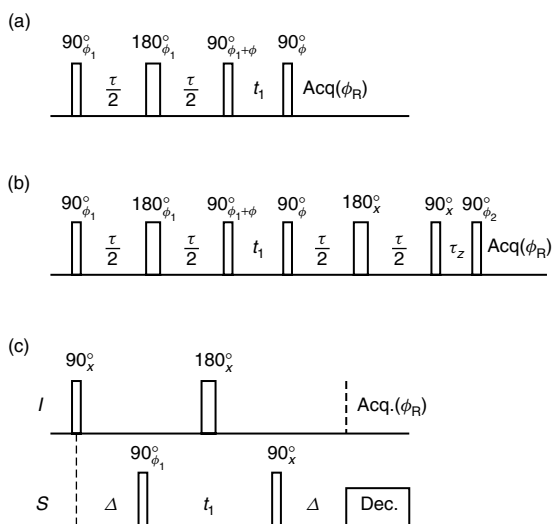


Figure 17.1. Pulse sequences for (a) INADEQUATE, (b) a one-dimensional multiple quantum filter producing in-phase spectra, and (c) HMQC. For (b), data must be averaged over several values of τ_z . Phase cycling for p quantum filtration for (a) and (b) where applicable: $\phi = x$ for even and y for odd orders; $\phi_1 = k\pi/p$, where $k = 0, 1, 2, \dots, (2p - 1)$; $\phi_2 = 2p(x, y, -x, -y)$. For (a), $\phi_R = (x, -x)$, for (b) $\phi_R = (x, -x) + 2p(x, y, -x, -y)$. For (c), $\phi_1 = (x, -x)$; $\phi_R = (x, -x)$. The number before each bracketed phase cycle indicates the number of consecutive transients that are acquired with each step. Where a phase cycle is a linear combination of bracketed cycles, the phases calculated from each one are added together to obtain the phase to be used.

these have found widespread use. One of the earliest of these, and perhaps the most successful is two-dimensional INADEQUATE^{3,5} [Figure 17.1(a)] applied to natural abundance ^{13}C . The experiment produces spectra that correlate pairs of coupled ^{13}C nuclei, while removing the singlets from uncoupled ^{13}C spins that would otherwise dominate the spectrum. In this instance double quantum excitation is particularly efficient, since homonuclear single bond ^{13}C coupling constants are both uniform and relatively large (typically 40 Hz). Furthermore, due to low natural abundance, each double quantum coherence can be considered as arising from a two-spin system.

Excitation is achieved through the process

$$\begin{aligned}
 (I_{Az} + I_{Xz}) &\xrightarrow{90^\circ_x} -(I_{Ay} + I_{Xy}) \\
 &\xrightarrow{\tau} (2I_{Ax}I_{Xz} + 2I_{Xx}I_{Az}) \\
 &\xrightarrow{90^\circ_x} -(2I_{Ax}I_{Xy} + 2I_{Xx}I_{Ay})
 \end{aligned}$$

When $\tau = 1/(2J_{CC})$, pure double quantum coherence [equation (17.6)] is excited with maximum efficiency. The delay t_1 is systematically incremented in successive experiments to encode the double quantum evolution in the second dimension of the data set. The 90° pulse following the subsequent multiple quantum evolution period t_1 reconverts the double quantum coherence into antiphase single quantum coherence which is detected as it becomes in-phase. Orthogonal components of double quantum coherence can be detected by shifting the phase of the last pulse or, alternantly, all the pulses of the excitation sequence by 45° ; this enables absorptive phase sensitive spectra to be acquired.

An example of an INADEQUATE spectrum is given in Figure 17.2. In the spectrum each pair of coupled ^{13}C spins is correlated by a pair of peaks that occur at their single quantum frequencies in F_2 and at the sum of their rotating frame frequencies (their mutual double quantum frequency) in F_1 . Consequently, all pairs of correlation peaks are symmetrically disposed about the $\omega_1 = 2\omega_2$ skew diagonal. Peaks of this sort are sometimes referred to as “direct” correlation peaks.

When abundant nuclei such as ^1H are under study, a wide range of both coupling constants and spin systems are usually encountered. The optimum value of τ will now be $1/(4J)$ where J is the average value of a coupling constant. However, to avoid the excitation of components of antiphase double quantum coherence, which would result in the introduction of dispersive components into peaks in the spectrum, a shorter

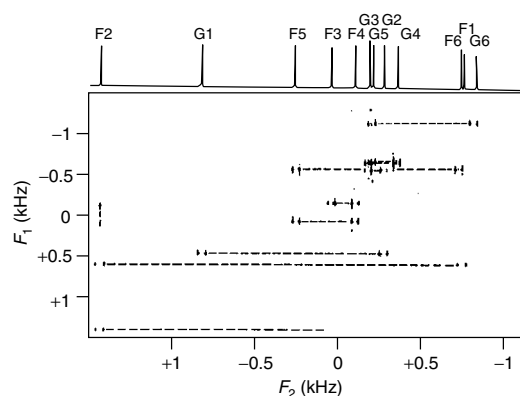


Figure 17.2. ^{13}C INADEQUATE spectrum of sucrose. (Reproduced by permission of Academic Press from A. Bax, R. Freeman, T. A. Frenkiel, and M. H. Levitt, *J. Magn. Reson.*, 1981, **43**, 478.)

value of τ must be used,³ typically $<1/(6J)$. This has the side effect of reducing peak intensity. The spectra so produced contain remote correlation peaks in addition to the direct ones described above. Remote peaks occur at the double quantum frequency of the pair of spins active in the double quantum coherence in F_1 and the single quantum frequency of a passive spin to which both active spins are coupled in F_2 .

A number of variations of the basic INAD-EQUATE pulse sequence have been introduced. Notable among these is a pair of experiments designed to produce spectra amenable to automated analysis.^{6,7} This is achieved by reducing the number of components present in the multiplet structure of the correlation peaks.

Of the other orders of coherence, both zero and triple quantum coherence have seen limited use. Zero quantum coherence is not amenable to the conventional method of achieving phase sensitive detection in the F_1 dimension, since it is insensitive to phase shifts, and consequently separate pulse sequences must be used.³ Furthermore, zero quantum spectra often contain intense peaks at $F_1 = 0$ arising from both coupled and uncoupled spins that cannot be removed by phase cycling. With triple and higher orders of coherence the major problems are reduced excitation efficiency and difficulty in exciting the single component of coherence necessary for producing absorptive spectra.

17.2.2 Heteronuclear Correlation Experiments

The most widely used heteronuclear multiple quantum correlation experiment is (see Chapter 22) HMQC^{3,8} (heteronuclear multiple quantum coherence) [Figure 17.1(c)]. This experiment produces absorptive phase sensitive spectra correlating the single quantum chemical shifts of pairs of coupled heteronuclei I and S , typically $^{15}\text{N}-^1\text{H}$ and $^{13}\text{C}-^1\text{H}$. The experiment and its derivatives are widely used to study ^{15}N and ^{13}C labeled proteins. The first two pulses excite heteronuclear zero and double quantum coherence:

$$\begin{aligned} I_z &\xrightarrow{90_x^0(I)} -I_y \xrightarrow{\Delta} [I_x \cos(\omega_I \Delta) + I_y \sin(\omega_I \Delta)] 2S_z \\ &\xrightarrow{90_x^0(S)} -[I_x \cos(\omega_I \Delta) + I_y \sin(\omega_I \Delta)] 2S_y \end{aligned}$$

where $\Delta = 1/(2J_{IS})$. Reconversion of the multiple quantum into in-phase single quantum coherence,

which is accomplished by the last $90^\circ(S)$ pulse and the subsequent delay, is the reverse of excitation. The $180^\circ(I)$ pulse at the center of the evolution period interconverts components of heteronuclear zero and double quantum coherence and reverses the effects of I spin chemical shift evolution during both Δ and t_1 intervals. This ensures that only S spin chemical shift is encoded by the IS zero quantum and double quantum coherence present during t_1 , and that when $t_1 = 0$ there is no offset-dependent phase shift of the observed magnetization.

Although multiple quantum coherence is used in this experiment to encode a single quantum chemical shift, it is usually preferred over purely single quantum alternatives because it requires only four pulses to do so, whereas the single quantum alternative would require 10. This means that HMQC requires less phase cycling and the smaller number of proton pulses makes solvent suppression easier.

The HMQC pulse sequence minus the first pulse is most widely used as a “module” that can be inserted into heteronuclear two-, three-, and four-dimensional experiments (see Chapter 25) to encode a heteronuclear chemical shift with the maximum efficiency and the minimum of phase cycling³ (often an important consideration). Many of these experiments have become central to the study of the solution structure of proteins by NMR.⁸

17.3 MULTIPLE QUANTUM EDITING EXPERIMENTS

Experiments that use multiple quantum coherence to produce spectra that are edited in some way can be grouped into two broad categories: multiple quantum filters that edit the spectrum solely on the basis of the orders of coherence that a spin can participate in and experiments that also use multiple quantum chemical shift, scalar couplings and spin coupling topologies as a basis for editing. In the former category, multiple quantum filtered COSY (see Chapters 12 and 13) and its derivative E.COSY (see Chapter 14) have entered general usage, while of the latter the DEPT experiment is most widely used.

17.3.1 Homonuclear One-dimensional Multiple Quantum Filtration

Any experiment that uses phase cycling or magnetic field gradient pulses to select a particular order of

coherence can be regarded as a multiple quantum filter. The first purpose-designed multiple quantum filter is the one-dimensional INADEQUATE⁹ experiment (Figure 17.2). Excitation and detection occur in the same way as for the two-dimensional INADEQUATE experiment described above, and the same considerations apply. However, unlike the two-dimensional experiment, the length of the evolution period t_1 is fixed at zero. This experiment produces double quantum filtered ^{13}C – ^{13}C satellite spectra from which the relatively intense peaks arising from uncoupled ^{13}C nuclei, beneath which satellite spectra are often undiscernible in the conventional single quantum spectrum, have been removed. It produces absorption spectra containing pairs of antiphase doublets that are easy to interpret.

However, problems arise when the technique is applied to ^{13}C enriched samples or to abundant nuclei such as ^1H . These are in many respects similar to the problems encountered in homonuclear multiple quantum correlation spectroscopy of abundant nuclei. As a consequence of the greater diversity of scalar coupling constants and spin systems, excitation becomes both less uniform and less efficient. Furthermore, filtered spectra produced with the INADEQUATE pulse sequence can be difficult to interpret since they may contain a superimposed mixture of absorptive and dispersive components that are antiphase with respect to different numbers of spins.

Relatively uniform excitation can be achieved, at the expense of efficiency, across coherences of a given order and across the different orders by setting $\tau = 1/(4J)$, where J is the average scalar coupling constant. Alternatively, the uniformity of excitation can be improved by combining spectra obtained with several different values of τ . However, to produce absorptive spectra it is necessary to modify the pulse sequence. The pulse sequence given in Figure 17.1(b) produces multiple quantum filtered spectra that are both absorptive and in-phase.³ After the two central 90° pulses which comprise the multiple quantum filter, antiphase single quantum coherence will be present. In the INADEQUATE experiment the magnetization is observed at this point, and consequently the peaks in the observed spectra will be antiphase. By contrast, in the modified pulse sequence a spin echo is introduced at this point to allow this antiphase magnetization to become in-phase again. The two 90° pulses at the end of the pulse sequence comprise a z filter¹ which serves to eliminate any remaining antiphase magnetization. Consequently, since only

in-phase magnetization will be present at the start of acquisition, the spectrum will also be in-phase.

When abundant nuclei are under study, nuclear magnetization can be filtered through other orders of coherence besides double quantum coherence; for nuclei of low natural abundance, sensitivity usually makes filtration through orders of coherence requiring more than two active spins impractical.

17.3.2 Multiple Quantum Filtered COSY

Multiple quantum filtered COSY^{10,11} is one of the most widely used multiple quantum experiments. Unlike one-dimensional filters it does not suffer from the problems of uniformity of excitation or mixing of absorptive and dispersive components in the observed spectrum; indeed, the phase properties are superior to those of the conventional COSY experiment (see Chapter 12). While filtration can, in principle, be through any order of coherence greater than one, in practice it is usually restricted to double quantum, and occasionally triple quantum, coherence since sensitivity declines as coherence order increases. The main motivation for using the experiment are a reduction in the intensity of diagonal peaks relative to off-diagonal peaks and the improvement in phase properties over conventional COSY referred to above.

Multiple quantum filtered COSY differs from its precursor in that the single 90° mixing pulse of the latter is replaced by a pair of pulses (Figure 17.3).

In the conventional COSY experiment a cross-correlation peak is generated between two spins k and l through coherence transfer between components of

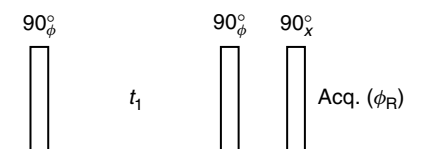


Figure 17.3. Pulse sequence for multiple quantum filtered COSY and E.COSY. For p quantum filtration $\phi = k\pi/p$, where $k = 0, 1, 2, \dots, (2p - 1)$; $\phi_R = (x, -x)$. An E.COSY spectrum can be generated by taking the linear combination of two quantum and three quantum filtered spectra: $\{\text{E.COSY}\} = \{2 \text{ quantum filtered COSY}\} + \frac{4}{3}\{3 \text{ quantum filtered COSY}\}$. In practice, E.COSY is acquired as a single experiment (see Chapter 14).

antiphase magnetization:

$$I_{kz} \xrightarrow{90_x^\circ} -I_{ky} \xrightarrow{t_1} 2I_{kx}I_{lz} \xrightarrow{90_y^\circ} -2I_{kz}I_{lx}$$

while autocorrelation peaks arise from components of magnetization that are in-phase when the mixing pulse is applied:

$$I_{kz} \xrightarrow{90_x^\circ} -I_{ky} \xrightarrow{t_1} -I_{ky} \xrightarrow{90_y^\circ} -I_{ky}$$

Clearly, since magnetization following the two pathways differ in phase by 90° , if one is phased to be absorptive than the other must inevitably be dispersive. If cross-correlation peaks are phased to be absorptive, as is usually the case, then the diagonal peaks will be dispersive. The dispersive tails of diagonal peaks often obscure adjacent cross-correlation peaks. In a multiple quantum filtered COSY experiment, all observed magnetization must pass through multiple quantum coherence of the selected order between the two mixing pulse. For example, in the case of double quantum filtered COSY,

$$I_{kz} \xrightarrow{90_x^\circ} -I_{ky} \xrightarrow{t_1} 2I_{kx}I_{lz} \xrightarrow{90_x^\circ} \frac{1}{2}(2I_{kx}I_{ly} + 2I_{ky}I_{lx})$$

$$\xrightarrow{90_y^\circ} \frac{1}{2}(2I_{kx}I_{lz} + 2I_{ky}I_{lx})$$

where only the selected components of coherence are shown. The second 90° pulse of the sequence actually creates $2I_{kx}I_{ly}$, which consists of a linear combination of zero quantum and double quantum coherence [equations (17.4) and (17.6)]; the linear combination of product operators given above corresponds to the pure double quantum coherence selected by the phase cycle. The two components of antiphase magnetization present after the mixing period give rise to the k spin autocorrelation peak (first term) and a $k-l$ cross-correlation peak (second term). Since both components have the same phase, both diagonal and off-diagonal peaks can be phased to be absorptive simultaneously, resulting in a spectrum consisting solely of absorption peaks. The main motivation for using double quantum filtration has, until recently, been to produce pure absorption COSY spectra with low intensity diagonal peaks. While double quantum filtration might, in principle, be used to remove the signal arising from water or other uncoupled-spin solvent peaks, in practice dynamic range problems and the limited efficiency of phase cycling has precluded this. However, the recent advent of actively shielded magnetic field gradients as a means

of coherence transfer pathway selection has now made solvent suppression practical as well. An example of a four quantum filtered COSY spectrum illustrating the technique's ability to produce edited spectra is given in Figure 17.4.

The structure of double quantum filtered COSY cross-correlation peaks is the same as in conventional COSY: they are antiphase with respect to the mutual coupling of the correlated spins in both dimensions. However, if filtration through higher orders of coherence is used, this will not be the case. In general, an

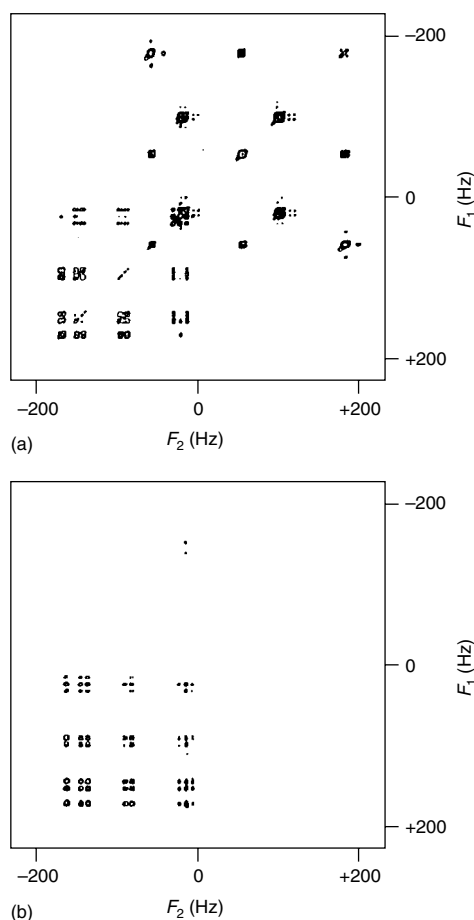


Figure 17.4. (a) 200 MHz COSY and (b) four quantum filtered COSY spectra of a mixture of 2,3-dibromothiophene, 2-furoic acid and 1-bromo-3-nitrobenzene in acetone- d_6 . Only the signals from 1-bromo-3-nitrobenzene are allowed to pass by the four quantum filter. (Reproduced by permission of Academic Press from A. J. Shaka and R. Freeman, *J. Magn. Reson.*, 1983, **51**, 169.)

n quantum filtered COSY cross-correlation peak will be antiphase with respect to $(n - 2)$ couplings in both dimensions of the spectrum in addition to the mutual coupling of the correlated spins. This is because the magnetization of a spin and n quantum coherence can only be interconverted by a nonselective pulse if the former is antiphase with respect to $(n - 1)$ other spins.

17.3.3 E.COSY

The overlap present in the one-dimensional spectra of all but the smallest molecules often makes the measurement of scalar coupling constants difficult. In principle, scalar coupling constants can be measured from the cross-correlation peaks of COSY spectra. However, in practice the limited digital resolution of two-dimensional experiments and the wide lines of larger molecules can both lead to the overlap of multiplet components, making analysis difficult. The E.COSY¹² experiment (see Chapter 14) alleviates this problem by taking advantage of the fact that much of the information present in cross-correlation peaks is redundant. A cross-correlation peak arising from a set of N mutually coupled spins will contain 2^{2N-1} components. E.COSY reduces this number to 2^N by restricting coherence transfer to transitions directly connected in the energy level diagram. A scalar coupling constant can be extracted from E.COSY spectra simply by measuring the distance between a pair of peaks without the need for any fitting procedure. E.COSY uses the same pulse sequence as multiple quantum filtered COSY, but with a different phase cycle. It effectively combines two, three, and sometimes four quantum filtered COSY spectra in the ratio 1:2:4. As noted in the previous section, the antiphase structure of a COSY cross-correlation peak will vary depending on the order of coherence that it is filtered through. Consequently, if different orders of multiple quantum filtered COSY spectra are combined in the appropriate ratios, some components will cancel out. E.COSY combines multiple quantum filtered COSY spectra in such a way that components which are not the result of coherence transfer between directly connected transitions cancel out. This is represented diagrammatically in Figure 17.5.

The E.COSY cross-peak structure is based on a series of displaced squares. A cross-correlation peak between two spins k and l at (ω_k, ω_l) will consist of a square antiphase with respect to the mutual coupling

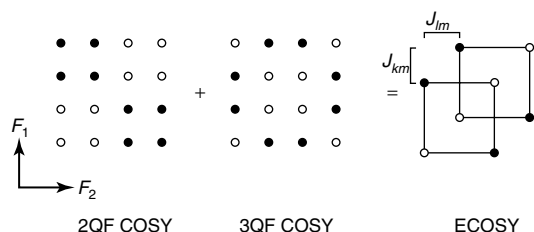


Figure 17.5. Representation of the generation of an E.COSY cross-correlation peak from a linear combination of two quantum (2QF) and three quantum filtered (3QF) COSY cross-correlation peaks. The correlation is from a spin k to a spin l . Both spins are also coupled to a third spin m . J_{km} and J_{lm} can be measured as the displacement of the two squares in F_1 and F_2 , respectively.

of the two spins in both dimensions. Each additional spin m to which both k and l are coupled will cause this square to be duplicated and displaced by (J_{km}, J_{lm}) . To determine J_{km} and J_{lm} it is only necessary to measure the displacement of the two squares in F_1 and F_2 , respectively (Figure 17.5). It has recently been shown that differential relaxation between components of in-phase and antiphase magnetization can give rise to substantial errors in the values of poorly resolved scalar coupling constants measured from E.COSY spectra.¹³

17.3.4 n -Spin Filtration

An n quantum filter passes magnetization from spin systems containing n or more spins. An n -spin filter^{3,14} is an n quantum filter modified so that it only passes magnetization from spin systems which contain exactly n spins. It consists of a multiple quantum filter with a multiplicity filter inserted into the multiple quantum evolution period. An n quantum coherence arising from a system of more than n spins will not be a singlet and consequently will be rejected by the multiplicity filter. The multiplicity filter consists of a spin echo of variable length. Data acquired with a number of echo times are coadded: the signals from singlets will not evolve during the echo and will therefore constructively interfere when combined, while nonsinglets will evolve due to their scalar couplings and will therefore destructively interfere. For complete cancellation of nonsinglets to occur, a wide range of echo times must be used. In practice, cancellation may be incomplete if there is

a transition at the center of the multiplet, which will not evolve during the echo, or two transitions closely spaced about the center.

17.3.5 Spin Topology Filtration

The most sophisticated type of homonuclear ^1H editing experiment yet developed is the spin topology filter.¹⁵ Filters of this type pass the magnetization of a single type of spin system. In essence, spin topology filters function by passing a particular order of coherence arising from a specific spin system. To achieve specificity it is often necessary to use a sophisticated multiple stage excitation sequence. These typically consist of a series of spin echoes sandwiched between 90° pulses. Selectivity is typically determined by the phases of the 90° pulses and the lengths of the spin echoes. The former restricts the coherence transfer process that can occur, while the latter allows manipulation of the scalar coupling evolution of intermediate coherences. The pulse sequence for AX_3 spin filtered COSY is given in Figure 17.6, and an experimental example is given in Figure 17.7.

In practice, spin topology filters can be difficult to implement and are very sensitive to variations in scalar coupling constants. This latter fact manifests itself in the presence of several peaks arising from the non- AX_3 spin systems in the example. Furthermore, long phase cycles are often required, and relaxation during the filter may result in a substantial reduction in signal intensity, precluding application to many biomolecules.

17.3.6 Heteronuclear Editing Experiments

Most heteronuclear multiple quantum editing experiments are designed to edit ^{13}C spectra on the basis

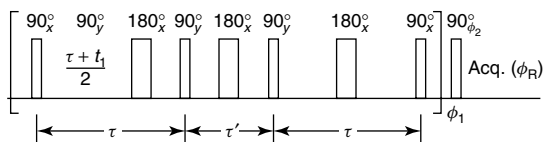


Figure 17.6. Pulse sequence for AX_3 spin filtered COSY.¹⁵ $\tau = 1/(2J)$ and $\tau' = 1/(6J)$. The phases ϕ , ϕ_1 , and ϕ_R are cycled to select ± 4 quantum coherence between the last two pulses.

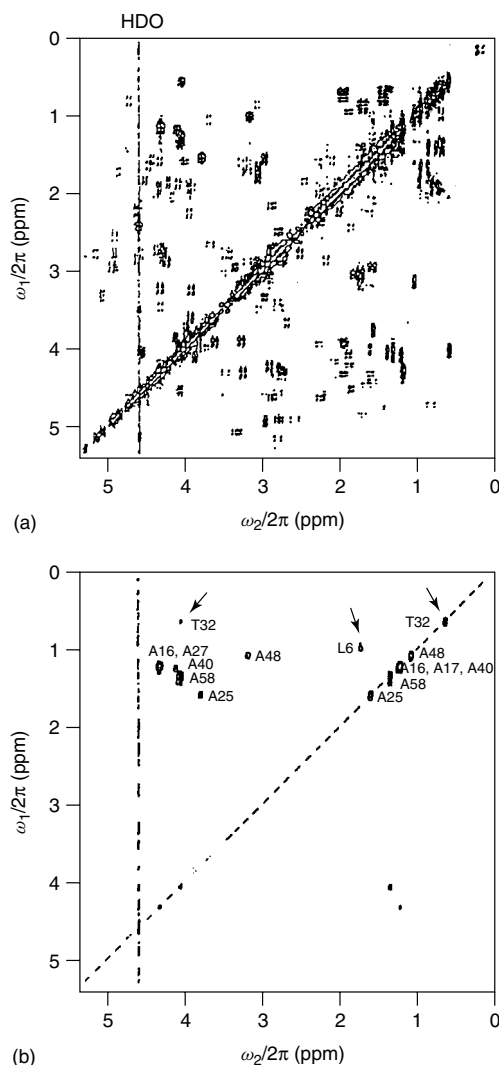


Figure 17.7. 300 MHz ^1H spectra of bovine trypsin inhibitor: (a) double quantum filtered COSY spectrum; (b) AX_3 spin filtered COSY spectrum. The peaks in (b) are predominantly due to alanines which have AX_3 spin systems.¹⁵ (Reproduced by permission of the American Institute of Physics from M. H. Levitt and R. R. Ernst, *J. Chem. Phys.*, 1985, **83**, 3297.)

of the number of attached protons. All make use of the relative uniformity of one bond carbon–proton couplings and the scalar coupling properties of multiple quantum filters. Multiple quantum filtration is also used in some experiments.

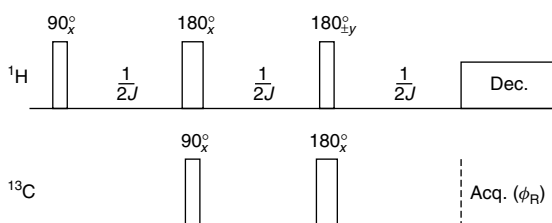


Figure 17.8. Pulse sequence for the DEPT experiment.¹⁶ Edited $^{13}\text{CH}_n$ subspectra can be obtained by combining data acquired with different three values of θ : $\theta_1 = 45^\circ$, $\theta_2 = 90^\circ$, and $\theta_3 = 135^\circ$. Subspectra are generated by taking the following linear combinations: CH, θ_2 ; CH_2 , $0.5(\theta_1 - \theta_3)$; CH_3 , $0.5[0.5(\theta_1 + \theta_3) - 0.71\theta_2]$.

The earliest and most widely used of the heteronuclear multiple quantum editing technique is the DEPT¹⁶ experiment (Figure 17.8). This experiment edits the response from different $^{13}\text{CH}_n$ groups into separate subspectra. Its effect is sketched in the product operator formalism:

$$\begin{aligned}
 & \text{H}_z \xrightarrow{90_x^{\circ}(\text{H})} -\text{H}_y \xrightarrow{[1/(2^1 J_{\text{CH}})]} 2\text{H}_x\text{C}_z \xrightarrow{90_y^{\circ}(\text{C})} 2\text{H}_x\text{C}_x \xrightarrow{[1/(2^1 J_{\text{CH}})]} \\
 & \text{CH} : 2\text{H}_x\text{C}_x \\
 & \text{CH}_2 : 4\text{H}_x\text{C}_y\text{H}_z \xrightarrow{\theta_y^{\circ}(\text{H})} -4\text{H}_z\text{C}_y\text{H}_z \sin\theta \cos\theta \\
 & \text{CH}_3 : 8\text{H}_x\text{C}_x\text{H}_z\text{H}_z \xrightarrow{\theta_y^{\circ}(\text{H})} 8\text{H}_z\text{C}_x\text{H}_z\text{H}_z \sin\theta \cos^2\theta
 \end{aligned}$$

The 180° pulses serve to reverse chemical shift evolution during the pulse sequence. After the first two pulses, heteronuclear zero and double quantum coherence between attached ^1H and ^{13}C nuclei is created from ^1H magnetization. Since scalar couplings between active spins are ineffective, the multiple quantum coherence evolves during the subsequent period solely due to its scalar couplings to passive spins, becoming (ideally) completely antiphase with respect to the remaining passive protons attached to the active carbon atom. This is then converted into ^{13}C magnetization antiphase with respect to all of its attached protons by the $\theta_y^{\circ}(\text{H})$ pulse, and is observed in the presence of proton decoupling once it has become in-phase. The efficiency of the last coherence transfer process is dependent upon both the angle θ and the type of $^{13}\text{CH}_n$ group. Consequently, by combining data acquired with three different values of θ it is possible to produce separate subspectra of CH, CH_2 , and CH_3 groups. DEPT is susceptible to errors if the values of θ are mis-set. This problem is circumvented in a variation of DEPT known as POMMIE¹⁷ in which $^{13}\text{CH}_n$ group selection is achieved with a multiple quantum filter instead of a flip angle filter.

The type of editing used in DEPT is taken a step further in two families of experiments known as SEMINA and SLAP.¹⁸ While DEPT edits for $^{13}\text{CH}_n$ groups, these experiments produce subspectra which are edited according to the type of $^{13}\text{CH}_m$ $^{13}\text{CH}_n$ group to which the ^{13}C nuclei belong. Like DEPT, these experiments rely on the generation of intermediate multiple quantum coherence and use flip angle filters to achieve editing. Spectra can be edited either according to the individual values of m and n , or, more usually, according to the parities of $(m+n)$ and m or n .

17.4 DETERMINATION OF THE SIGN OF SCALAR COUPLING CONSTANTS

The properties of multiple quantum coherence provide several opportunities for determining the relative signs of scalar coupling constants. While it might be expected that this information would be accessible from their scalar coupling properties, it is perhaps more surprising that in some circumstances their relaxation rates can also be used.

It can be seen from equation (17.2) that the scalar couplings exhibited by multiple quantum coherences are sensitive to the signs of scalar coupling constants. For example, a zero quantum coherence with active spins k and l will exhibit a scalar coupling of $(J_{km} - J_{lm})$ to a passive spin m . Consequently, if the zero quantum coupling is equal to the difference in magnitudes of the two scalar coupling constants their signs must be the same; otherwise, the converse must be true. For the corresponding double quantum coherence this situation is reversed.³

When a pair of spin- $1/2$ nuclei are scalar coupled to a common quadrupolar nucleus, the relative signs of these two coupling constants can be determined from the scalar contribution to the relaxation of the zero and double quantum coherences in which the two spin- $1/2$ nuclei are active.¹⁹ If the spin- $1/2$ nuclei are k and l , and the quadrupolar nucleus is S , then

$$\begin{aligned}
 1/T_2(\text{DQC/ZQC}) &= 1/T_1(k) + 1/T_1(l) \\
 &\quad + \frac{4}{3}N_S\pi^2S(S+1) \\
 &\quad \times (J_{kS} \pm J_{lS})^2T_1(S) \quad (17.7)
 \end{aligned}$$

where N_S is the number of S spins and $T_1(k)$ is the T_1 value of the k spin. Clearly, if the zero quantum coherence relaxes more quickly than the double quantum coherence, the scalar coupling constants must

have the same sign, while if the reverse is true they must have opposite signs. It should be noted that this expression is an approximation; it is assumed that the dipolar relaxation of k and l makes a relatively small contribution to the overall relaxation rate.

17.5 CORRELATION OF EXTERNAL RANDOM MAGNETIC FIELDS

The interaction of molecules with each other is of great chemical and biochemical interest. When one molecule is paramagnetic it may induce random magnetic fields at the nuclei in the other, contributing to their relaxation. By measuring the transverse relaxation times of zero and double quantum coherence it is possible to determine the extent to which the random magnetic fields induced in this way are correlated for the active spins, and consequently to investigate the interaction between the two molecules.²⁰

If two weakly coupled spin- $1/2$ nuclei k and l are considered to relax solely with external random magnetic fields, their single quantum transverse relaxation rates will be

$$1/T_2(k) = \gamma^2 \tau_c [\overline{B_{lx}^2} + \overline{B_{kx}^2} + \overline{B_{kz}^2}] \quad (17.8)$$

$$1/T_2(l) = \gamma^2 \tau_c [\overline{B_{kx}^2} + \overline{B_{lx}^2} + \overline{B_{lz}^2}] \quad (17.9)$$

where B_{ij} corresponds to the j component of the external field experienced by the nucleus i . While the relaxation rates of both coherences are sensitive to the external random fields experienced by both nuclei, they are not sensitive to any correlation between them. The corresponding relaxation rates for the zero and double quantum coherences in which these spins are active are

$$1/T_2(\text{ZQC}) = \gamma^2 \tau_c [\overline{B_{kx}^2} + \overline{B_{lx}^2} + \overline{B_{kz}^2} + \overline{B_{lz}^2} - 2C_{kl}(\overline{B_{kz}^2} \overline{B_{lz}^2})^{1/2}] \quad (17.10)$$

$$1/T_2(\text{DQC}) = \gamma^2 \tau_c [\overline{B_{kx}^2} + \overline{B_{lx}^2} + \overline{B_{kz}^2} + \overline{B_{lz}^2} + 2C_{kl}(\overline{B_{kz}^2} \overline{B_{lz}^2})^{1/2}] \quad (17.11)$$

where C_{kl} is a correlation coefficient. Clearly, both these coherences are sensitive to any correlation in the external random magnetic fields experienced by the two nuclei through the term $2C_{kl}(\overline{B_{kz}^2} \overline{B_{lz}^2})^{1/2}$. Since it reduces the rate of zero quantum relaxation and increases that of double quantum coherence, any correlation will manifest itself as a difference between the two rates. From this difference the extent of correlation can be determined.

RELATED ARTICLES IN THE ENCYCLOPEDIA OF MAGNETIC RESONANCE

Double Quantum Coherence

INADEQUATE Experiment

Multiple Quantum Coherence Imaging

Multiple Quantum Coherence in Spin-1/2 Dipolar Coupled Solids

Multiple Quantum Coherences in Extended Dipolar Coupled Spin Networks

Multiple Quantum NMR in Solids

Phase Cycling

REFERENCES

1. R. R. Ernst, G. Bodenhausen, and A. Wokaun, *Principles of Nuclear Magnetic Resonance in One and Two Dimensions*, Clarendon, Oxford, 1987.
2. M. Munowitz, *Coherence and NMR*, Wiley, New York, 1988.
3. T. J. Norwood, *Progr. NMR Spectrosc.*, 1992, **24**, 295.
4. O. W. Sørensen, G. W. Eich, M. H. Levitt, G. Bodenhausen, and R. R. Ernst, *Progr. NMR Spectrosc.*, 1983, **16**, 163.
5. A. Bax, R. Freeman, and T. A. Frenkiel, *J. Am. Chem. Soc.*, 1981, **103**, 2102.
6. S. Wimperis, *J. Magn. Reson.*, 1990, **87**, 174.
7. M. Novic, H. Oschkinat, P. Pfaendler, and G. Bodenhausen, *J. Magn. Reson.*, 1987, **73**, 493.
8. G. M. Clore and A. M. Gronenborn, *Progr. NMR Spectrosc.*, 1991, **23**, 43.
9. A. Bax, R. Freeman, and S. P. Kempsell, *J. Am. Chem. Soc.*, 1980, **102**, 4849.
10. U. Piantini, O. W. Sørensen, and R. R. Ernst, *J. Am. Chem. Soc.*, 1982, **104**, 6800.
11. A. J. Shaka and R. Freeman, *J. Magn. Reson.*, 1983, **51**, 169.
12. C. Griesinger, O. W. Sørensen, and R. R. Ernst, *J. Am. Chem. Soc.*, 1985, **107**, 6394.
13. T. J. Norwood and K. Jones, *J. Magn. Reson., Ser. A*, 1993, **104**, 106.
14. D. S. Williamson, D. L. Nagel, R. S. Markin, and S. M. Cohen, *J. Magn. Reson.*, 1987, **71**, 163.

15. M. H. Levitt and R. R. Ernst, *J. Chem. Phys.*, 1985, **83**, 3297.
16. D. M. Doddrell, D. T. Pegg, and M. R. Bendall, *J. Magn. Reson.*, 1982, **48**, 323.
17. J. M. Bulsing and D. M. Doddrell, *J. Magn. Reson.*, 1985, **61**, 197.
18. N. C. Nielsen, H. Bildsoe, H. J. Jackobsen, and O. W. Sørensen, *J. Magn. Reson.*, 1988, **78**, 223.
19. V. Mlynarik, *Chem. Phys. Lett.*, 1989, **160**, 25.
20. A. Wokaun and R. R. Ernst, *Mol. Phys.*, 1978, **36**, 317.

